ACS OMEGA

Open Access

http://pubs.acs.org/journal/acsodf

Article

Polaron Formation in Conducting Polymers: A Novel Approach to Designing Materials with a Larger NLO Response

Atazaz Ahsin,[#] Iqra Ejaz,[#] Sehrish Sarfaraz, Khurshid Ayub,[*] and Haitao Ma[*]

Cite This: *ACS Omega* 2024, 9, 14043−14053

Read Online

ACCESS | Metrics & More | Article Recommendations

ABSTRACT: Substantial efforts have been made to design and investigate new approaches for high-performance nonlinear optical (NLO) materials. Herein, we report polaron formation in conducting polymers as a new approach to designing materials with a large NLO response. A comparative study of polypyrrole and polypyrrole-based polaron (nPy^+ where n = 1, 3, 5, 7, and 9) is carried out for optoelectronic and NLO properties. The studied polarons (PPy^+) show excellent electronic properties and have reduced ionization potential (IP) as compared to neutral PPy, and a monotonic decrease is observed with increased chain lengths (**1Py** to **9Py**). Interesting trends of global reactivity descriptors can be seen; the softness (S) increases with an increase in the chain length of PPy, while the hardness (η) decreases in the same fashion. The $E_{H\text{-}L}$ gaps for the PPy^+ polaronic state are significantly lower than their corresponding neutral PPy. In the polaronic model (PPy^+), radicals decisively reduce the crucial excitation energy, reminiscent of excess electrons (alkali metals). The performed TDOS spectral analysis further justifies the better conductive and electronic properties of polarons (PPy^+) with increased chain lengths (conjugation). The static hyperpolarizability response (β_o) is recorded up to 1.3×10^2 au for **9Py**, while for polaron $9Py^+$, it has increased up to 3.2×10^4 au. The static hyperpolarizability of the $9Py^+$ polaronic state is 246 times higher than that of the corresponding neutral analogue, **9Py**. It is observed that the values of β_o obtained at the CAM-B3LYP/6-311+G(d,p) level of theory are comparable to those obtained at the LC-BLYP and ωB97XD functionals. The β_{vec} values show a strong correlation with the total hyperpolarizability (β_o). Furthermore, the calculated second harmonic generation (SHG) values are up to 4.0×10^6 au at 532 nm, whereas electro-optic Pockel's effect (EOPE) is much more pronounced at the smaller dispersion frequency (1064 nm). The TD-DFT study reveal the red-shifted absorption maxima (λ_{max}) with an increased length of PPy^+. A significant reduction in excitation energy (ΔE) is observed with increased length of PPy and PPy^+, which also favors the improved NLO response. Hence, the studied thermally conducting polypyrrole-based polarons (PPy^+) are new entries into NLO materials with better electrical and optical features.

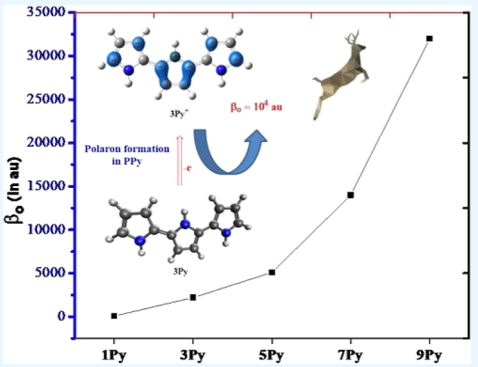

INTRODUCTION

Materials possessing nonlinear optical (NLO) properties change the propagation characteristics (polarization, phase, frequency, amplitude, etc.) of light.[1] Nonlinear optics has found many applications in the communications, photonics industries, data storage, and computer display technology.[2−6] The early examples of NLO materials were based on inorganic materials; however, organic NLO materials have gained much interest recently due to their chemical flexibility and variety of synthetic strategies.[7,8] Several strategies have been proposed to enhance the nonlinear optical (NLO) response, which include the electron push−pull mechanism,[9] donor−acceptor-π-conjugation (D-π−A) strategy,[10] bond length alternation (BLA),[11] multidecker sandwich complexes,[12] diradical character,[13] octupolar molecules,[14] and the excess electron system via doping.[15,16]

The doping of metals (1st and second groups) to inject excess electrons into materials is a quick approach to enhance NLO response in both (inorganic and organic) systems.[17,18] A metal atom is doped on the substrate (doped material), where its excess electrons are diffused into the system and reduce the excitation energy of the system, which ultimately increases the first hyperpolarizability (β_o).[19] Several systems containing electropositive metals as external dopants on the homo and heteroatomic inorganic nanocages[20] and fullerenes have been reported.[21] Kosar et al. have investigated the effect of doping single and multialkali metal@C_{24} complexes for NLO applications, where the $Na_3@C_{20}$ complex has the highest β_o value of 2.74×10^5 au.[18] Similarly, Maria et al. explored alkali metal-doped boron and aluminum phosphide nanocages for

Received: November 27, 2023
Revised: January 25, 2024
Accepted: March 7, 2024
Published: March 18, 2024

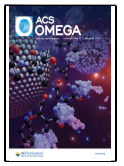

NLO properties, where hyperpolarizability shows dependence on the size of alkali metals.[17] Very recently, our group proposed single alkali metal-containing nonconventional alkalides based on M@[12-crown4] and M@[12-crown-5] for electronic and NLO properties.[22] In this study, a noticeable hyperpolarizability value (β_o = up to 1.2 × 10^7 au) was reported for Li@[15-crown-5], which is attributed to the presence of loosely bound excess electrons.[22] A large number of studies were presented which demonstrate that excess electrons are crucial in promoting the static and dynamic NLO responses of clusters and molecules[23,24,25].

Excess electron compounds, or clusters, are those which contain extra transferable (excitable) electrons, which just look like Rydberg orbitals.[26] These excess electrons are the type of unique anions with dispersivity, loose binding, and other intriguing properties that play a critical role in decreasing the excitation energies (during crucial transition).[27] The reduction in HOMO−LUMO gaps is the driving force that makes excitation easier in the crucial transition.[28] In earlier research, Dye's group succeeded in providing the first experimental evidence of excess electron compounds in 1983 for the synthesized Cs^+(18-crown-6)2e compound, which has characteristics of electride (alkali metal bearing a negative charge).[29]

Unpaired electrons (single radicals) behave in a similar way to alkali metals, and one expects an enhancement in the NLO properties of such radical species. Recent studies have demonstrated that unpaired electrons in orbitals (lying in the plane) and their spin multiplicity might be responsible for electronic and NLO properties.[30,31] These unpaired electrons are known as radical systems, and they function similarly to excess electrons inside molecules. For a variety of organic radical systems, Nakano et al. investigated the impacts of spin multiplicity, basis set, and electron correlation, which affect the NLO coefficients.[32]

Theoretically, polarons carry a spin (±1/2) and are radical cations that can be designed by removing an electron from the conducting polymers. Also, it was investigated that increasing the size of the polarons (chain length) would improve the electrical and conductive properties. The unpaired electrons (radicals) in conducting polymers are responsible for the tunable electronic and conducting properties. Introducing a single cation charge in conjugated polymers would form polarons, whereas the bicationic state is described as bipolarons. Polarons have a very low excitation energy, as evidenced by the reported UV−visible spectra. The low excitation energy can result in a remarkable NLO response due to a nonlinear electric field interaction. This prompted us to explore polarons for the NLO properties. We became interested in studying the polaronic state of polypyrrole for its hyperpolarizability response.

Polypyrroles (PPy) are one of the most intensively studied conducting polymers due to their simple and inexpensive preparation, along with their widely admitted character as good sensors, actuators, and solar cell materials.[33,34] Conducting polymers are characterized by alternate double and single bonds and have tremendous applications in interdisciplinary science.[35] Since neutral polypyrrole has a broadband gap and makes it difficult to move electrons from the valence band to the conduction band, it is considered to be an insulator. Due to their radical nature, PPy^+ carries an unpaired electron, which might play a crucial role in evaluating electronic, optical, and NLO properties. Therefore, theoretical modeling of polypyrrole-based polarons (PPy^+) can be interesting for investigating electronic and NLO properties. Using polaron-based PPy (which resembles excess electrons) compounds reduces the excitation energy significantly, enhancing electronic and NLO properties. We performed a comparative study to investigate the role of polarons in improving the intrinsic properties of polypyrrole (PPy). Using DFT, we considered nPy (n = 1, 3, 5, 7, and 9) in neutral and cation (polarons). We mainly focused on the role of polarons in the conjugated polymer (PPy) and the change in their properties from the intrinsic to the polaronic state. The NLO properties of PPy are evaluated through polarizabilities (α), hyperpolarizabilities (β_o), and dynamic hyperpolarizabilities $\beta(\omega)$.

Computational Details. All the quantum chemical calculations were performed using the CAM-B3LYP method with a 6-31+G (d,p) basis set using the g09 software.[36] First, we considered the 1 to 9 units of pyrrole rings, and optimization was performed at CAM-B3LYP without any symmetry constraints. CAM-B3LYP is a hybrid exchange−correlation function that includes the hybrid properties of the B3LYP functional and the long-range corrected Coulomb attenuating method (CAM) parameter. B3LYP is a hybrid part of the above method that contains Beckes 3-parameters for the exchange functional and Lee- Yang-parr- correlation functional (LYP). The performance of CAM-B3LYP is reliable for atomization energies and charge transfer-excitation.[37] It is also demonstrated by Limacher et al.,[38] that CAM-B3LYP provides accurate results for molecular geometry, much closer to experimental results.

After optimization, frequency calculations are performed to confirm that these structures are true minima on the potential energy surface (PES). Dipole moment, FMO analysis, and HOMO−LUMO ($E_{H\text{-}L}$) gaps are calculated at the same level of theory. Furthermore, we have calculated electronic properties and global reactivity of the studied nPy, which include the ionization potential (IP), electronic affinity (EA), chemical hardness (η), chemical softness (S), and chemical potential (χ) given by the following relations.

$$\text{ionization potential (IP)} = -E_{\text{HOMO}} \tag{1}$$

$$\text{electron affinity (EA)} = -E_{\text{LUMO}} \tag{2}$$

$$\text{chemical hardness } (\eta) = \frac{1}{2}(\text{IP} - \text{EA}) \tag{3}$$

$$\text{chemical softness (S)} = \frac{1}{2\eta} \tag{4}$$

$$\text{chemical potential } (\chi) = -(\text{IP} + \text{EA})/2 \tag{5}$$

Nonlinear optical properties are induced by asymmetric charge displacements that are generated under the influence of light. The energy of the perturbed system is described by the Taylor expansion

$$E = E^O - \mu_I F_i - \left[\frac{1}{2!}\right]\alpha_{ij}F_iF_j - \left[\frac{1}{3!}\right]\beta_{ijk}F_iF_jF_k - \left[\frac{1}{4!}\right]\gamma_{ijkl}F_iF_jF_kF_l \tag{6}$$

Polarizability (α_o) and first hyperpolarizability (β_o) values of PPy and polaron (PPy^+) are studied at the same level of theory with the 6-31+G(d,p) basis set. This level of theory is reliable for the estimation of polarizability (α_o), first hyperpolarizability (β_o), and other electronic parameters.[39,40] In the previous

https://doi.org/10.1021/acsomega.3c09468
ACS Omega 2024, 9, 14043−14053

studies, several types of hyperpolarizability values, such as β_{vec}, β_o, and β_{HRS}, were computed through this approach. We adopted the coupled-perturbed Kohn–Sham (CPKS) method to calculate the hyperpolarizability.

$$\mu = \sqrt{\mu_X^2 + \mu_Y^2 + \mu_Z^2} \tag{7}$$

$$\alpha_{ij} = \left(\frac{\delta\mu_i}{\delta F_j}\right)_{E_{\to 0}} \tag{8}$$

$$\alpha_{tot} = \frac{1}{3}(\alpha_{xx} + \alpha_{yy} + \alpha_{zz}) \tag{9}$$

The magnitude of hyperpolarizability can be defined as

$$\beta_x = \beta_{xxx} + \beta_{xyy} + \beta_{xzz}$$

$$\beta_y = \beta_{yyy} + \beta_{yxx} + \beta_{yzz}$$

$$\beta_x = \beta_{zzz} + \beta_{zxx} + \beta_{zyy}$$

$$\beta_{tot} = \sqrt{\beta_x^2 + \beta_y^2 + \beta_z^2} \tag{10}$$

The frequency-dependent NLO response is also calculated by the same method at applied frequencies of 532 and 1064 nm. In this regard, we estimated electro-optical Pockel's effect (EOPE) and second harmonic generation (SHG) phenomena. Time-dependent density functional theory (TD-DFT) simulations were considered at TD-CAM-B3LYP for getting excited state parameters. We considered 40 excited states (singlet and triplet), and a crucial excited state (highest oscillator strength) was adopted to determine absorbance (λ_{max}), excitation energies (ΔE), and oscillator strength), which is used to get the values of oscillator strength (f_o) and excitation energies (ΔE). To get a clear picture of the electronic properties of the studied PPy, we performed a total density of state (TDOS) analysis by using GaussSum software.[41]

RESULTS AND DISCUSSION

Optimized Geometries of (PPy and PPy$^+$). Initially, optimized geometries of polypyrrole (PPy) at the CAM-B3LYP/6-31+G (d,p) functional are shown in Figure 2. We have considered the odd number of nPy (up to 9 units) for our investigation. The largest oligomers up to nine units (9Py) and their corresponding polarons (9Py$^+$), which represent the structural properties of polypyrrole (PPy), are considered. The optimized geometries of neutral PPy are depicted in Figure 2. Figure 1 shows the neutral and radical generation of the **3Py** unit. All the neutral nPy have the C_1 point group symmetry with planar structures. On the other hand, the optimized structures of polypyrrole-based polarons (PPy$^+$) are almost planar, and no distortions in the geometries were seen. The obtained point group symmetry for PPy$^+$ is C_1, the same as that for their corresponding neutral PPy. Several important geometric parameters (bond angle, bond length, and dihedral angles) are computed for PPy$^+$, and values are given in Table 1.

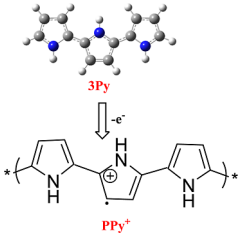

Figure 1. Representation of 3Py and 3Py$^+$.

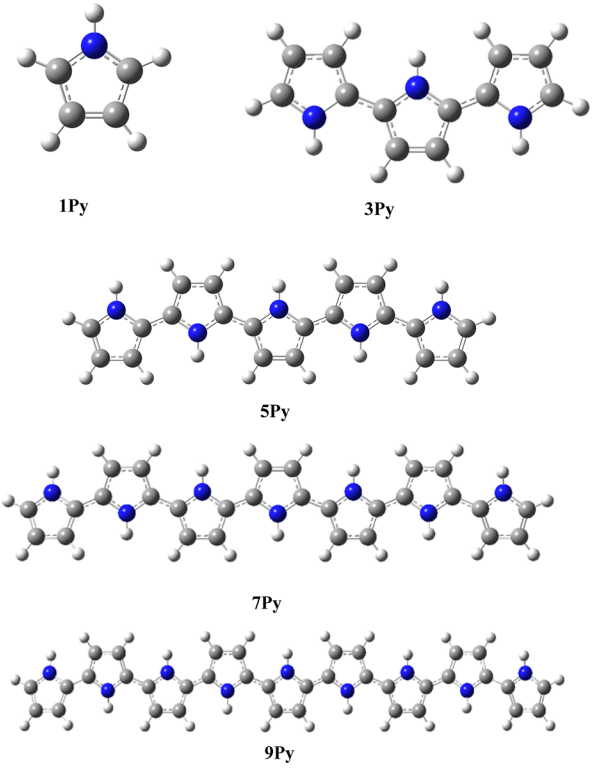

Figure 2. Optimized geometries of polypyrrole (PPy) at the CAM-B3LYP/6-31+G(d,p) level of theory; blue color indicates the N atom, while gray one for carbon atoms.

Table 1. Symmetries, Average Bond Lengths (in Å), and Bond Angles (∠ C–N–C/C–C–C/H–C–C/H–N–C in Degree) of Polypyrrole-Based Polarons (PPy$^+$)

nPy	L_{C-C}	L_{C-N}	L_{C-H}	(∠ C–N–C)	(∠C–C–C)	(∠H–C–C)
1Py$^+$	1.43	1.36	1.08	109.07	107.15	128.06
3Py$^+$	1.42	1.38	1.08	109.07	107.15	128.06
5Py$^+$	1.43	1.38	1.08	109.07	107.15	128.06
7Py$^+$	1.44	1.38	1.08	109.07	107.15	128.06
9Py$^+$	1.45	1.38	1.08	109.07	107.15	128.06

In the studied PPy$^+$, 4-types of bond lengths are present, namely: C–C, C–H, N–C, and N–H. The C–C bond length lies in the range of 1.43 to 1.39 Å, while the computed C–N bond length (L_{C-N}) ranges from 1.36 to 1.39 Å in these polarons. The measured carbon and hydrogen bond distances (L_{H-C}) are identical to those for neutral PPy and range from 1.09 to 1.07 Å. The C–N bond lengths (L_{C-N}) slightly increased with an increase in conjugation and chain lengths (1Py$^+$ to 9Py$^+$). Vibrational frequency analysis of polarons and neutral PPy reveals that they are true minima on the potential energy surface, since no negative frequency is associated. For polarons, the measured average bond angles of C–N–C, C–C–C, and H–C–C are 109.07°, 107.15°, and 128.06°, respectively. On the other hand, the average bond angle of H–N–C is 125.47°. The computed average dihedral angles in

https://doi.org/10.1021/acsomega.3c09468
ACS Omega 2024, 9, 14043–14053

Table 2. Spin Densities of the Studied Polypyrrole-Based Polarons (nPy^+)

$1Py^+$		$3Py^+$		$5Py^+$		$7Py^+$		$9Py^+$	
C1	0.555	C2	0.14	C1	0.16	C1	0.13	C1	0.12
C2	0.555	C1	0.22	C2	0.12	C2	0.10	C2	0.08
N	−0.129	C3	0.21	C3	0.13	C3	0.11	C3	0.09
		C4	0.21	C4	0.13	C4	0.10	C4	0.05
		N5	−0.07	N5	−0.06	C5	0.10	C5	0.06
		C6	0.14	C6	0.12	C6	0.13	C6	0.09
		C7	0.22	C7	0.17	N1	−0.05	C7	0.08
						N2	−0.03	C8	0.12
								N1	−0.05
								N2	−0.03

PPy^+ for N−C−C−N and C−C−C−C are 177.92° and −168.87°, respectively (Table 1).

Spin Densities of Polypyrrole-Based Polarons (PPy^+). The distribution of the unpaired spin density is crucial for determining the electronic properties of our studied PPy and PPy^+. The calculated spin densities are listed in Table 2 and Figure 3. One can observe the reduction in spin densities with an increased chain length of PPy^+. The obtained spin densities for $1Py^+$ are higher and lie on the carbon atom of the PPy^+ ring. The higher value of spin density is obtained for $1Py^+$. It can be observed that the spin density decreases over the larger PPy^+ rings, and spin densities are dramatically reduced for corner rings. For $1Py^+$, the radical (unpaired) electrons are lying at C1 and C2, whereas for $3Py^+$, the spin densities are higher at the middle ring and are slightly reduced for terminal rings. Likewise, thesities for $5Py^+$ are also higher in the case of the central Py-ring, and radicals (unpaired electrons) are associated with C3 and C4 for $5Py^+$. Likewise, the spin density on $7Py^+$ was reduced to 0.10, and the maximum for the central ring was reduced to C3 and C4 (Figure 3). For $9Py^+$, the values of spin densities are further reduced to 0.05, and overall, density is higher at the middle ring and becomes negligible for the terminal Py^+-rings. The performed spin density analysis concludes that the highest spin density is in the middle of these polypyrrole rings. Radical (unpaired electron) formation can be seen to be delocalized over the central PPy^+ rings, and its delocalization rises with greater conjugation (chain length), where values of spin densities also decrease.

Electronic Properties and Global Reactivity. The electronic stability of the studied PPy and polarons (PPy^+) is verified by the calculated ionization potential (IP) and vertical electron affinity (EA). The ionization potential and electron affinity are calculated by using Koopman's theorem approximation.[42] The negative HOMO is taken as the ionization potential (IP), whereas the negative LUMO energy is considered the electron affinity (EA). The calculated values of IP and EA of neutral and polaronic PPy are given in Table 3. From the given values (Table 3), the IP values for neutral PPy are smaller than those of polaronic PPy^+ and lie in the range of 7.36 to 5.67 eV. The values decreased with an increased chain length of PPy. On the contrary, for polarons (PPy^+), the values are significantly increased and lie in the range of 14.75 to 7.83 eV, where the lowest value was observed for $9PPy^+$. Similarly, the EAs values for neutral PPy range from −0.77 to −0.24 eV, whereas for polaronic PPy^+, these values are quite higher and range from 4.98 to 2.98 eV. In the polaronic state, there is a significant reduction in EA values with the increased chain length and conjugation of polypyrrole. PPy^+ shows positive electron affinity and might be an electron acceptor undergoing charge transfer reactions, whereas negative electron affinity values are associated with neutral PPy.

The reactivity and stability of these structures were also evaluated through global reactivity descriptors. In this regard, we computed the chemical hardness (η), chemical potential (χ), and softness (s). The computed results of the global reactivity descriptors are given in Table 3. The resistance of a molecule's electron distribution to change is assessed by its hardness (η). For neutral PPy, the η values decreased with increasing chain length, where the lowest value (2.17 eV) accounts for **9Py**. For the PPy^+, a slightly increased chemical hardness (η) can be seen, ranging from 4.89 to 2.43 eV. The chemical softness of neutral PPy ranges from 0.15 to 0.23 eV, and values slightly increased for **1P** to **9Py**. The softness of polaron (PPy^+) is slightly smaller than that of neutral PPy, and there is a monotonic increase in softness with the increased chain length of polypyrrole. Moreover, we have calculated the chemical potential (χ) of PPy and PPy^+, and the values are given in Table 3. The chemical potential (μ) outlines the escaping tendency of electrons from an equilibrium system. The values of χ are calculated by eq 5, which is given in the methodology section. The stability of polypyrrole (PPy) is shown by the negative chemical potential values; nPy are stable and do not spontaneously split. The values of χ for neutral nPy range from −3.29 to −2.66 eV, and there is a gradual decrease in values from **1Py** to **5Py** and then slightly increased to −2.71 eV for **9Py**. On the other hand, the χ values for polypyrrole polarons (PPy^+) are higher and range from −9.86 to −5.41 eV. Hence, PPy^+ offers better chemical stability based on their chemical potential values.

Orbital Analysis of PPy and PPy^+. The frontier orbital gap helps to characterize the chemical reactivity, kinetic stability, and optical polarizability of molecules. We carried out frontier molecular orbital analysis (FMOs) at the UCAM-B3LYP/6-31+G (d,p) level of theory. Additionally, the FMO study is used to predict the spread of the electronic density of the orbitals in the studied polypyrrole. The energies of the highest occupied molecular orbitals (HOMO) and lowest unoccupied molecular orbitals (LUMO) energies and their corresponding HOMO−LUMO gaps ($E_{H\text{-}L}$) are given in Table 4 for the neutral and polaronic states. In the neutral state, the HOMO−LUMO ($E_{H\text{-}L}$) gaps range from 8.13 to 5.91 eV, where the lowest $E_{H\text{-}L}$ value is recorded for **9Py**, and the highest value is observed for **1Py**. The significant reduction in the $E_{H\text{-}L}$ gaps may be attributed to the increased conjugation in PPy.

On the other hand, the HOMO−LUMO gaps for polarons PPy^+ are slightly higher than the neutral polymers (PPy), and values range from 9.77 to 4.85 eV (Table 4). These values are

https://doi.org/10.1021/acsomega.3c09468
ACS Omega 2024, 9, 14043−14053

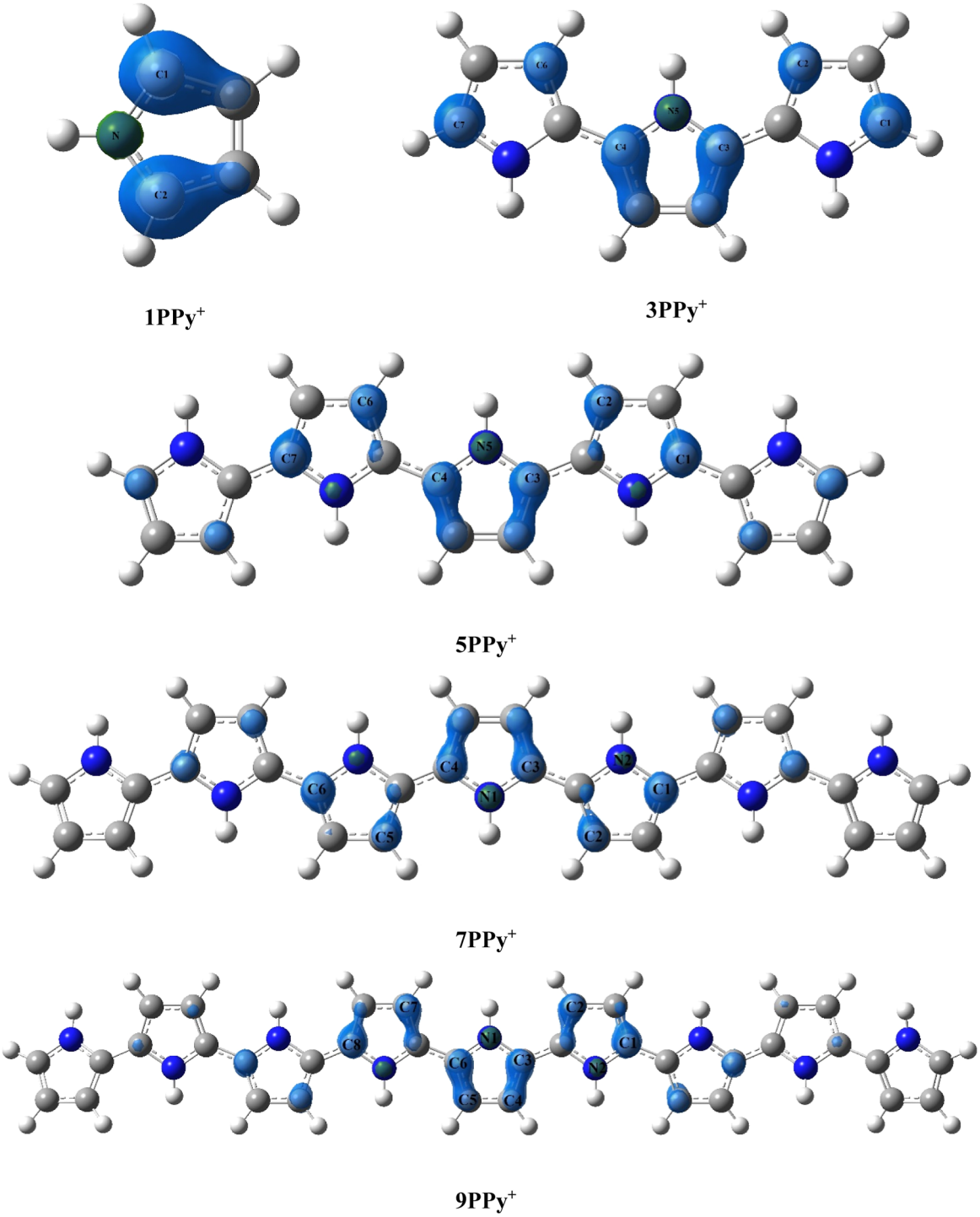

Figure 3. Spin densities of polypyrrole polarons (PPy^+) at isovalue 0.005.

Table 3. Ionization Potential (IP in eV), Electron Affinity (VEA in eV), Chemical Hardness (η in eV), Chemical Softness (S in eV), and Chemical Potential (χ in eV) of PPy and PPy^+

	Neutral state (PPy)					Polaronic state (PPy^+)				
nPy	IP	EA	η	S	χ	IP	EA	η	S	χ
1Py	7.36	−0.77	3.29	0.15	−3.29	14.75	4.98	4.89	0.10	−9.86
3Py	5.98	−0.52	2.73	0.18	−2.91	10.12	3.92	3.13	0.16	−7.02
5Py	5.84	−0.42	2.71	0.18	−2.66	8.84	3.40	2.72	0.18	−6.15
7Py	5.74	−0.31	2.71	0.18	−2.71	8.24	3.12	2.56	0.19	−5.68
9Py	5.67	−0.24	2.17	0.23	−2.71	7.83	2.98	2.43	0.20	−5.41

https://doi.org/10.1021/acsomega.3c09468
ACS Omega 2024, 9, 14043−14053

Table 4. HOMO and LUMO Energies and HOMO − LUMO (E_{H-L}) Gaps (in eV) for Neutral and Polaronic PPy

	Neutral state (PPy)			Polaronic state (PPy^+)		
Polymer	HOMO	LUMO	E_{H-L}	HOMO	LUMO	E_{H-L}
1Py	−7.36	0.77	8.13	−14.75	−4.98	9.77
3Py	−5.98	0.52	6.54	−10.12	−3.92	6.21
5Py	−5.84	0.42	6.26	−8.84	−3.406	5.43
7Py	−5.74	0.31	6.05	−8.24	−3.12	5.12
9Py	−5.67	0.24	5.91	−7.83	−2.98	4.85

monotonically decreased from 1Py + to 9Py+, guaranteeing excellent electronic and conductive properties. From $1Py^+$ to $3Py^+$, the E_{H-L} value dramatically decreases, and $9Py^+$ displays a smaller gap than the corresponding 9Py. For the polypyrrole-based polaronic model (PPy^+), the decreasing sequence of HOMO−LUMO gaps is $1Py^+ > 3Py^+ > 5Py^+ > 7Py^+ > 9Py^+$. Furthermore, 9Py's substantial HOMO energy (−7.83 eV) makes it possible to observe the reduced E_{H-L}. The increased chain length of **9Py**$^+$ has a radical (unpaired electron), which can be excited easily from HOMO to LUMO and would result in improved electrical and conductive properties. The higher degree of conjugation would also result in a drastic increase in the conductivity and reactivity of polypyrrole-based polarons. The density of the HOMO and LUMO orbitals is shown in Figure 4. The HOMO density cloud lies on the entire rings of PPy, whereas the LUMO is shifted into the middle of the rings, which shows the presence of unpaired electrons (radical). The correlation between the spin density and the existence of electronic density on the central rings in PPy^+ justifies the availability of radicals.

Static Nonlinear Optical (NLO) Properties. The literature is rich in describing different materials' NLO responses based on their hyperpolarizability values. Several studies were presented, which unfold the crucial role of excess electrons in triggering the NLO properties of molecules and clusters[25,43,16,15]. For the first time, we studied the role of unpaired electrons (single radical) in conducting NLO-response polymers.

On the other hand, the formation of polarons in polypyrrole (oligomers) and their effect on electronic and NLO properties have still not been explored. Hence, the presence of radicals (polarons) shows a resemblance to excess electrons in determining the optical and NLO properties. The polarizability (α_o) of neutral PPy lies in the range of 50 to 6.0×10^2 au, where the highest value is obtained for **9Py**, while the lowest value is for **1Py**. The polarizability (linear response) values increase gradually from **1Py** to **9Py** with an increased chain length of the polypyrrole. Likewise, the α_o values for polarons (PPy^+) are quite higher and range from 42 to 2.7×10^3 au (Table 5). The presence of polaron-doped polypyrrole significantly increases the polarizability of PPy. The $9Py^+$ complex is 4.5 times more polarizable than the neutral **9Py**.

To further explore the NLO response of polypyrrole, we calculated the hyperpolarizability (β_o) values for second-order electric susceptibility (χ^2). The β_o values for neutral PPy range from 57 to 1.3×10^2 au, where the highest hyperpolarizability is found for **9Py**, while the lowest value is observed for **1Py** (Table 5). The increased chain length and conjugation result in a drastic increase in β_o values for PPy.

On the other hand, interesting increased β_o values are observed for polarons (PPy^+), and the value increased up to 3.2×10^4 au for $9Py^+$. Strikingly, the β_o response for polaronic

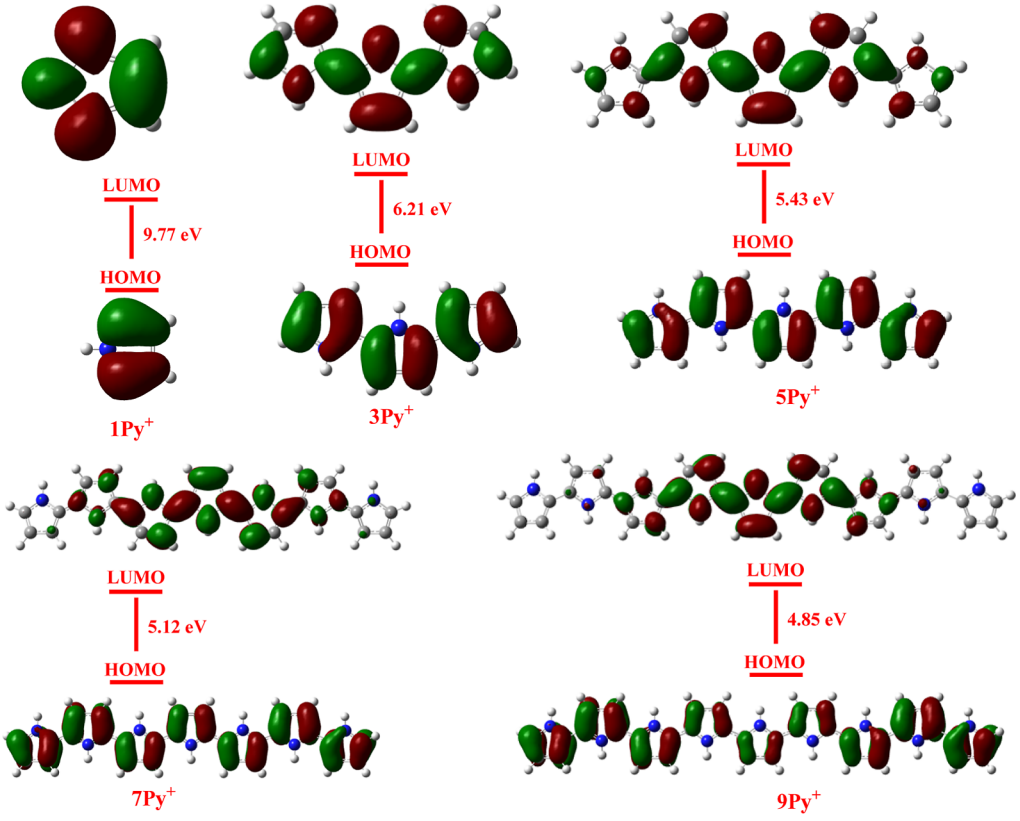

Figure 4. HOMO and LUMO densities of polarons (PPy^+) at the CAM-B3LYP (isovalue = 0.025).

https://doi.org/10.1021/acsomega.3c09468
ACS Omega 2024, 9, 14043−14053

Table 5. Static Polarizability (α_o in au), Static First Hyperpolarizability (β_o in au), Static Second Hyperpolarizability (γ_o in au), and β_{vec} and Dipole Moment (μ) of PPy and PPy^+

	Neutral state (PPy)			Polaronic State (PPy^+)		
PPy	α_o	β_o	β_{vec}	α_o	β_o	β_{vec}
1Py	50	57	57	42	6.1×10^1	6.1×10^1
3Py	1.7×10^2	1.0×10^2	1.0×10^2	2.4×10^2	2.2×10^3	2.6×10^3
5Py	3.1×10^2	3.4×10^2	2.3×10^2	6.6×10^2	5.1×10^3	4.2×10^3
7Py	4.5×10^2	2.0×10^2	2.0×10^2	1.5×10^3	1.4×10^4	1.4×10^4
9Py	6.0×10^2	1.3×10^2	1.3×10^2	2.7×10^3	3.2×10^4	3.1×10^4

Table 6. Calculated Mean Polarizabilities, α_o (au) and Mean First Hyperpolarizabilities, β_o (au) on CAM-B3LYP, LC-BLYP, and WB97XD of Polypyrrole-Based Polarons (PPy^+) as Well as for Alkyl Polypyrrole-Based Polarons (R-PPy^+)

	CAM-B3LYP		LC-BLYP		wB97XD			CAM-B3LYP	
nPPy	α_o	β_o	α_o	β_o	α_o	α_o	R-nPPy$^+$	α_o	β_o
1PPy$^+$	42	6.1×10^1	38	1.2×10^1	38	8.7×10^1	**R-1PPy$^+$**	71	8.8×10^1
3PPy$^+$	2.4×10^2	2.2×10^3	2.3×10^2	3.8×10^3	2.2×10^2	2.6×10^3	**R-3PPy$^+$**	3.0×10^2	2.6×10^3
5PPy$^+$	6.6×10^2	5.1×10^3	7.1×10^2	3.4×10^3	6.7×10^2	5.3×10^3	**R-5PPy$^+$**	7.7×10^2	8.7×10^3
7PPy$^+$	1.5×10^3	1.4×10^4	1.5×10^3	2.4×10^4	1.5×10^3	1.5×10^4	**R-7PPy$^+$**	1.5×10^3	9.3×10^3
9PPy$^+$	2.7×10^3	3.2×10^4	2.4×10^3	3.1×10^4	2.6×10^3	3.0×10^4	**R-9PPy$^+$**	2.7×10^3	1.4×10^4

Table 7. Static Hyperpolarizability (β_o in au), Frequency-dependent Hyperpolarizability $\beta(\omega)$ in Terms of Electro-Optic Pockel's Effect (EOPE) β ($-\omega$; ω, 0) in au, and Electric Field-Induced Second Harmonic Generation $\beta(-2\omega;\omega,\omega)$ in au at ω = 532 and 1064 nm of PPy^+

	ω = 0	ω = 532 nm		ω = 1064 nm	
nPy$^+$	β (0; 0,0)	β ($-\omega$; ω,0)	$\beta(-2\omega; \omega,\omega)$	β ($-\omega$; ω,0)	β (-2ω; ω, ω)
1Py$^+$	6.2×10^1	2.1×10^1	7.0×10^1	1.7×10^2	1.9×10^1
3Py$^+$	2.8×10^3	2.4×10^3	3.4×10^4	5.4×10^3	1.7×10^3
5Py$^+$	6.1×10^3	1.4×10^4	7.7×10^4	4.8×10^5	1.0×10^6
7Py$^+$	1.4×10^4	5.8×10^4	4.0×10^6	6.1×10^3	1.3×10^4
9Py$^+$	3.2×10^4	5.5×10^4	1.8×10^5	1.3×10^4	1.7×10^4

$9Py^+$ is 24.6 times higher than that of neutral **9Py**, which might be attributed to the presence of a radical (unpaired electron) in polypyrrole-based polarons. Hyperpolarizability (β_o) increases with the chain lengths in these polarons. Electronic properties can be correlated with hyperpolarizability responses, where a reduced ionization potential favors improved NLO properties as chain length grows. Similarly, the correlation of the electronic properties of PPy^+ with the electronic parameters can be seen by analyzing IP, HOMO − LUMO (E_{H-L}) gaps, and chemical hardness (η). The decreased values of IPs and E_{H-L} would result in a significant enhancement in the β_o response. Hence, based on the thermal stability of PPy, a drastic change in their electronic properties can be seen by introducing the polaron model. The designed polypyrrole-based polarons are the new candidate in NLO materials based on their superb electronic and static hyperpolarizability response.

Additionally, to further explore the NLO properties, we estimated the projection of hyperpolarizability on the dipole moment (β_{vec}). The values of the vector part of hyperpolarizability are given in Table 5. An identical trend of β_{vec} with β_o can be seen in the studied polypyrrole and their corresponding polarons (PPy^+), which suggests the projection of hyperpolarizability on the dipole moment vector in one direction. A nice correlation is observed between β_o and β_{vec}, indicating that hyperpolarizability lies mainly on the dipole moment axis in the unidirection.

Moreover, polarizability and hyperpolarizability values are also calculated on other DFT functionals for comparison (LC-BLYP and WB97XD functional) with the 6-31+G(d,p) basis set (see Table 6). The obtained results are compared with results observed at the CAM-B3LYP/6-31+G(d,p) level of theory. Overall, it is observed that the values of β_o obtained at the CAM-B3LYP/6-311+G(d,p) level of theory are comparable to those obtained at the LC-BLYP and WB97XD functionals. These additionally computed results support and validate our results computed initially at the CAM-B3LYP/6-311+G(d,p) level of theory. Moreover, we introduced the alkyl (propyl) chain at the N−H groups of pyrrole rings and calculated their NLO response. The calculated values for polypyrrole-based polarons with an alkyl chain (R-PPy+) are reported in Table 6. The comparison of the obtained mean polarizabilities (α_o) and mean first hyperpolarizabilities (β_o) of polypyrrole-based polarons with an alkyl chain (R-PPy+) with the polypyrrole-based polarons (PPy^+) reveals that the NLO response is almost comparable. The polarizabilities and first hyperpolarizabilities values in both cases vary by ±0.1 au.

Dynamic NLO Properties of Polarons. As polarons (PPy^+) have excellent static NLO properties, we extended our study to frequency-dependent NLO properties. The dynamic hyperpolarizability $\beta(\omega)$ values have been reported with incident frequencies of 532 and 1064 nm. The molecular design of highly active dynamic nonlinear optical (NLO) materials has been a hot topic in materials science because of their future applications in photonics and optoelectronics. The $\beta(\omega)$ is estimated through electro-optical Pockel's effect (EOPE) β ($-\omega$; ω, 0) and second harmonic generation (SHG) $\beta(-2\omega; \omega, \omega)$ phenomenon. The frequency-depend-

https://doi.org/10.1021/acsomega.3c09468
ACS Omega 2024, 9, 14043−14053

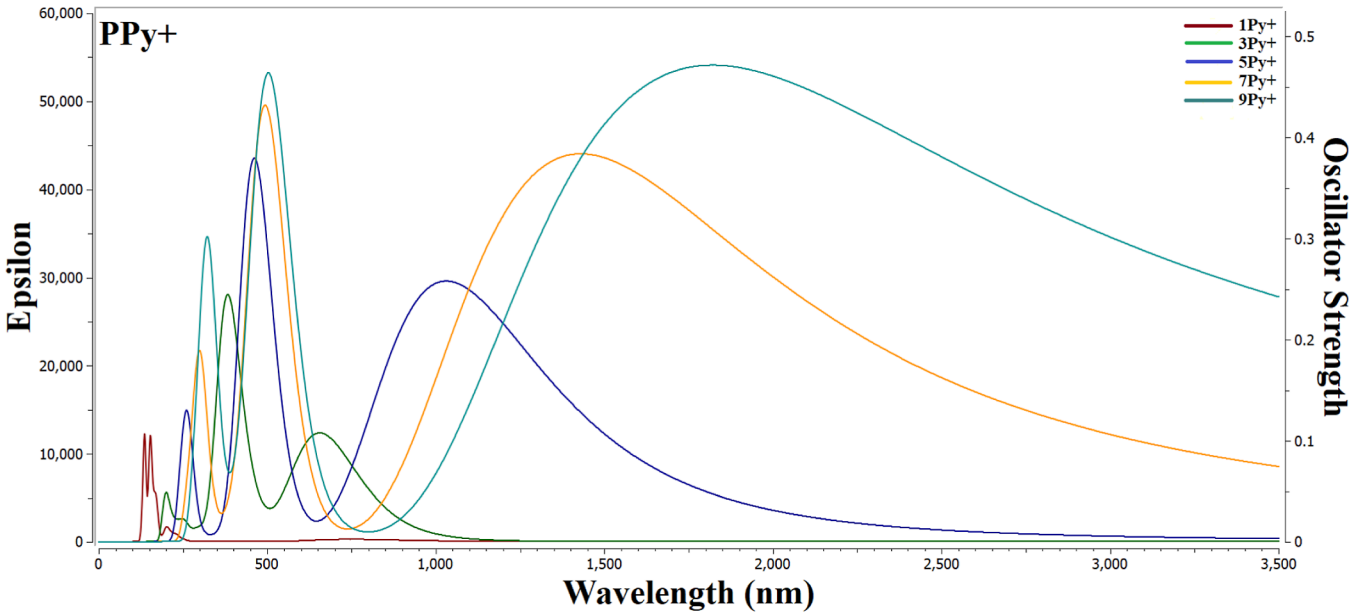

Figure 5. Absorption spectra of polypyrrole-based polarons (PPy^+) at the TD-CAM-B3LYP/6-31 + g(d,P) method.

ent NLO parameters are given in Table 7. The light with specific wavelengths of 532 nm (ω = 0.0856 au) and 1064 nm (ω = 0.0428 au) was adopted for simulations. Overall, the simulated frequency-dependent first hyperpolarizabilities $\beta(\omega)$ are quite higher than that of static hyperpolarizability (β_o). The increased $\beta(\omega)$ response indicates external frequency's role in polypyrrole's nonlinearity. The determined EOPE and SHG values are significant at smaller dispersion frequency of 1064 nm (0.0428 au), whereas the values are slightly reduced at the frequency of 532 nm (Table 7). The calculated β ($-\omega$, ω, 0) value of 5.5×10^4 au is the highest for **9Py$^+$** at 532 nm, while it increased up to 4.8×10^5 au for **5Py$^+$** with reduced external frequency (1064 nm). Likewise, the calculated significant SHG value of 4.0×10^6 au is recorded for **7Py$^+$** at 532 nm, while it became 1.0×10^6 au for **5Py$^+$** at the dispersion frequency of 1064 nm.

UV−visible Study of Polarons. The NLO materials are unique because they have a second harmonic generation (SHG) doubling frequency. Materials with the highest NLO qualities must be transparent in the presence of a functioning laser. The UV−visible properties of polypyrrole-based polarons (PPy^+) are evaluated using TD-DFT calculations, and the spectra are shown in Figure 5. Table 8 shows the results of absorption wavelengths, total energy, and maximal oscillator strengths (during the crucial transition). In polarons (PPy^+), the absorbance spectra are red-shifted, and band gaps are reduced. The absorption maxima of PPy appear in the range of 200 to 1800 nm, whereas the highest absorption of 9Py$^+$ was recorded at 1821 nm. The calculated absorption maxima (λmax) values for **1Py$^+$**, **3Py$^+$**, **5Py$^+$**, and **7Py$^+$** are 149, 377, 463, and 1430 nm, respectively. The modest absorption in the UV−visible region is observed in these maximums, demonstrating appropriate transparency under a generally practical laser. The **1Py$^+$**, in particular, is transparent in the deep UV region of (200 nm). As a result, these findings show that these polymers can serve as crucial building blocks for deep-violet NLO materials.

Table 8. Transition Energies (ΔE) in au, Oscillator Strength (f_o in au), and Absorption Wavelengths (λmax in nm, Dipole Moments (μ in au) for all Polypyrrole-Based Polarons

nPy$^+$	ΔE	f_o	λ_{max}	μ
1Py$^+$	8.29	0.29	149	0.73
3Py$^+$	3.28	0.59	377	0.76
5Py$^+$	2.67	1.07	463	0.74
7Py$^+$	0.88	1.08	1430	0.75
9Py$^+$	0.68	1.34	1821	0.76

Density of States (DOS) Analysis of Polarons (PPy^+). Total density of states analysis (TDOS) was used to get further insights into the studied polarons' electronic properties and orbital energies. The density of states (DOS) is the number of different states that electrons can occupy at a particular energy level. The formation of new energy states and alterations in the intensity of their peaks in the density of states (DOS) spectra are crucial for understanding the interaction mechanism and conductive properties of these polymers. The plotted TDOS spectra are shown in Figure 6. From the plotted spectra, one can observe that an increased number of PPy^+ rings would increase the number of states that appeared. The newly born energy states are also shifted to higher energy, which is also responsible for the significant reduction in HOMO−LUMO gaps. For 1PPy$^+$ the HOMO line appears near −10 eV, and for higher 9PPy$^+$, the HOMO energy line rose to near 5 eV. Hence, the increased conjugation and chain length of PPy^+ would result in enhanced electrical and conductive properties. Thus, the larger-sized polarons (PPy^+) show better conductive and nonlinear optical properties.

CONCLUSIONS

We presented a new approach to designing PPy-based polarons with remarkable electronic and NLO properties. The formation of polarons in thermally conducting polymers (PPy) has significantly reduced excitation energies (ΔE), which would result in a drastic enhancement in static first hyperpolarizability (β_o). The studied polarons (PPy^+) show excellent electronic properties and have reduced ionization

https://doi.org/10.1021/acsomega.3c09468
ACS Omega 2024, 9, 14043−14053

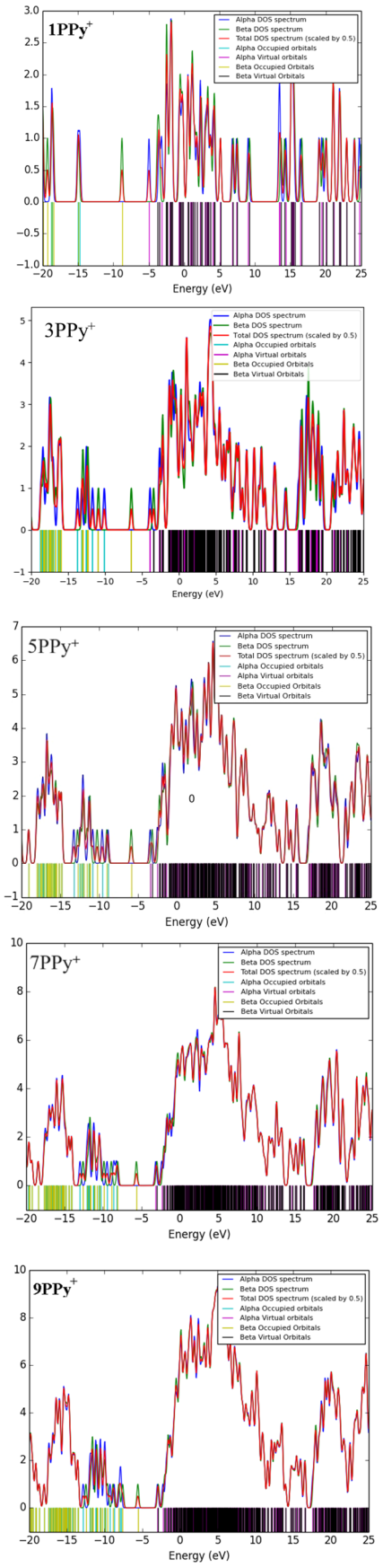

Figure 6. TDOS spectra of polarons (PPy^+).

potential (IP) as compared to neutral PPy, and values decrease further with increased chain lengths (**1Py** to **9Py**). The global reactivity descriptors show an interesting trend where softness (S) grows with the PPy chain length but hardness (η) decreases in the same fashion. The $E_{H\text{-}L}$ gaps for the PPy^+ polaronic state are significantly lower than their corresponding neutral PPy. In the polaronic model (PPy^+), radicals decisively reduce the crucial excitation energy reminiscent of excess electrons (alkali metals). The static hyperpolarizability response (β_o) is recorded up to 1.3×10^2 au for **9Py**, while for polaron $9Py^+$, it has risen up to 3.2×10^4 au. The static hyperpolarizability of the $9Py^+$ polaronic state is 246 times higher than the corresponding neutral analogue, **9Py**. The β_{vec} values show a strong correlation with the total hyperpolarizability (β_o). The performed TDOS spectral analysis further justifies the better conductive and electronic properties of polarons (PPy^+) with increased chain lengths (conjugation). Furthermore, the calculated second harmonic generation (SHG) values are up to 4.0×10^6 au at 532 nm, whereas electro-optic Pockel's effect (EOPE) is much more pronounced at a higher dispersion frequency (1064 nm). The TD-DFT study further shows the increased absorption maxima (λ_{max}) with the increased size of PPy^+. With increased length, a significant reduction in excitation energies (ΔE) is observed; PPy also favors the improved NLO response. Due to their improved thermal and electronic properties, the studied polypyrrole-based polarons (PPy^+) are novel additions to the NLO material family.

■ ASSOCIATED CONTENT

Data Availability Statement

The author affirms that the article's Supporting Information and the data used to support the study's findings are included. Upon a reasonable request, raw data from the corresponding sources are accessible to support the findings of this study.

■ AUTHOR INFORMATION

Corresponding Authors

Khurshid Ayub − *Department of Chemistry, COMSATS University Islamabad, Abbottabad Campus, Abbottabad KPK, 22060, Pakistan;* orcid.org/0000-0003-0990-1860; Email: khurshid@cuiatd.edu.pk

Haitao Ma − *Beijing National Laboratory for Molecular Sciences, Institute of Chemistry, Chinese Academy of Sciences, Beijing 100190, China;* orcid.org/0000-0002-2506-5498; Email: mht@iccas.ac.cn

Authors

Atazaz Ahsin − *Beijing National Laboratory for Molecular Sciences, Institute of Chemistry, Chinese Academy of Sciences, Beijing 100190, China; School of Chemical Sciences, University of Chinese Academy of Sciences, Beijing 100049, China*

Iqra Ejaz − *Department of Chemistry, COMSATS University Islamabad, Abbottabad Campus, Abbottabad KPK, 22060, Pakistan*

Sehrish Sarfaraz − *Department of Chemistry, COMSATS University Islamabad, Abbottabad Campus, Abbottabad KPK, 22060, Pakistan*

Complete contact information is available at: https://pubs.acs.org/10.1021/acsomega.3c09468

https://doi.org/10.1021/acsomega.3c09468
ACS Omega 2024, 9, 14043−14053

Author Contributions

[#]These authors contributed equally to this work.

Notes

The authors declare no competing financial interest.

■ ACKNOWLEDGMENTS

The authors thank the Higher Education Commission of Pakistan and COMSATS University, Abbottabad Campus, for their financial and technical assistance. This work is supported by the Beijing Municipal Natural Science Foundation (no.8212043). We also thank to the Alliance of International Science Organizations.

■ REFERENCES

(1) Reichert, M.; Hu, H.; Ferdinandus, M. R.; Seidel, M.; Zhao, P.; Ensley, T. R.; Peceli, D.; Reed, J. M.; Fishman, D. A.; Webster, S.; et al. Temporal, spectral, and polarization dependence of the nonlinear optical response of carbon disulfide. *Optica* **2014**, *1*, 436−445.

(2) Koirala, K. P.; Garcia, H.; Sandireddy, V. P.; Kalyanaraman, R.; Duscher, G. Bimetallic Fe−Ag Nanopyramid Arrays for Optical Communication Applications. *Nano Mater.* **2021**, *4*, 5758−5767.

(3) Divya, M.; Malliga, P.; Pragasam, A. An Investigation on Opto-thermo-mechanical Behaviour of a Borate Family NLO Crystal for Photonic Applications. *Braz. J. Phys.* **2021**, *51*, 1625−1635.

(4) Anis, M.; Muley, G. G.; Hakeem, A.; Shirsat, M. D.; Hussaini, S. S. Exploring the influence of carboxylic acids on nonlinear optical (NLO) and dielectric properties of KDP crystal for applications of NLO facilitated photonic devices. *Opt. Mater.* **2015**, *46*, 517−521.

(5) Gounden, D.; Nombona, N.; Van Zyl, W. E. Recent advances in phthalocyanines for chemical sensor, non-linear optics (NLO) and energy storage applications. *Coord. Chem. Rev.* **2020**, *420*, 213359.

(6) Guo, J.; Huang, D.; Zhang, Y.; Yao, H.; Wang, Y.; Zhang, F.; Wang, R.; Ge, Y.; Song, Y.; Guo, Z.; et al. 2D GeP as a novel broadband nonlinear optical material for ultrafast photonics. *Laser Photonics Rev.* **2019**, *13*, 1900123.

(7) Ramajothi, J.; Dhanuskodi, S. Crystal growth, thermal and optical studies on phase matchable new organic NLO material for blue-green laser generation. *J. Cryst. Growth* **2006**, *289*, 217−223.

(8) Balaprabhakaran, S.; Chandrasekaran, J.; Babu, B.; Thirumurugan, R.; Anitha, K. Synthesis, crystal growth and physiochemical characterization of organic NLO crystal: L-ornithinium dipicrate (LODP). *Spectrochim. Acta, Part A* **2015**, *136*, 700−706.

(9) Elhorri, A. M. Theoretical study of new push−pull molecules based on transition metals for NLO applications and determination of ICT mechanisms by DFT calculations. *J. Theor. Comput. Chem.* **2020**, *19*, 2050026.

(10) Ooyama, Y.; Ito, G.; Kushimoto, K.; Komaguchi, K.; Imae, I.; Harima, Y. Synthesis and fluorescence and electrochemical properties of D−π-A structural isomers of benzofuro [2, 3-c] oxazolo [4, 5-a] carbazole-type and benzofuro [2, 3-c] oxazolo [5, 4-a] carbazole-type fluorescent dyes. *Org. Biomol. Chem.* **2010**, *8*, 2756−2770.

(11) Blanchard-Desce, M.; Alain, V.; Bedworth, P. V.; Marder, S. R.; Fort, A.; Runser, C.; Barzoukas, M.; Lebus, S.; Wortmann, R. Large Quadratic Hyperpolarizabilities with Donor−Acceptor Polyenes Exhibiting Optimum Bond Length Alternation: Correlation Between Structure and Hyperpolarizability. *Chem. - Eur. J.* **1997**, *3*, 1091−1104.

(12) Hatua, K.; Nandi, P. K. Beryllium-cyclobutadiene multidecker inverse sandwiches: Electronic structure and second-hyperpolarizability. *J. Phys. Chem. A* **2013**, *117*, 12581−12589.

(13) Fukuda, K.; Matsushita, N.; Minamida, Y.; Matsui, H.; Nagami, T.; Takamuku, S.; Kitagawa, Y.; Nakano, M. Impact of Diradical/Ionic Character on Third-Order Nonlinear Optical Property in Asymmetric Phenalenyl Dimers. *ChemistrySelect* **2017**, *2*, 2084−2087.

(14) Liu, Z.; Hua, S.; Wu, G. Extended first hyperpolarizability of quasi-octupolar molecules by halogenated methylation: whether the iodine atom is the best choice. *J. Phys. Chem. C* **2018**, *122*, 21548−21556.

(15) Zhong, R. L.; Xu, H. L.; Li, Z. R.; Su, Z. M. Role of excess electrons in nonlinear optical response. *J. Phys. Chem. Lett.* **2015**, *6*, 612−619.

(16) Ahsin, A.; Ayub, K. Superalkali-based alkalides Li3O@[12-crown-4]M (where M= Li, Na, and K) with remarkable static and dynamic NLO properties; A DFT study. *Mater. Sci. Semicond. Process.* **2022**, *138*, 106254.

(17) Iqbal, J.; Iqbal, J.; Ludwig, R.; Ayub, K. Phosphides or nitrides for better NLO properties? A detailed comparative study of alkali metal doped nano-cages. *Mater. Res. Bull.* **2017**, *92*, 113−122.

(18) Kosar, N.; Tahir, H.; Ayub, K.; Mahmood, T. DFT studies of single and multiple alkali metals doped C24 fullerene for electronics and nonlinear optical applications. *J. Mol. Graphics Modell.* **2021**, *105*, 107867.

(19) Maria, M.; Iqbal, J.; Ayub, K. Theoretical study of the non linear optical properties of alkali metal (Li, Na, K) doped aluminum nitride nanocages. *RSC Adv.* **2016**, *6*, 94228−94235.

(20) Cariati, E.; Macchi, R.; Roberto, D.; Ugo, R.; Galli, S.; Casati, N.; Macchi, P.; Sironi, A.; Bogani, L.; Caneschi, A.; et al. Polyfunctional inorganic− organic hybrid materials: an unusual kind of NLO active layered mixed metal oxalates with tunable magnetic properties and very large second harmonic generation. *J. Am. Chem. Soc.* **2007**, *129*, 9410−9420.

(21) Tahir, H.; Kosar, N.; Ayub, K.; Mahmood, T. Outstanding NLO response of thermodynamically stable single and multiple alkaline earth metals doped C20 fullerene. *J. Mol. Liq.* **2020**, *305*, 112875.

(22) Ahsin, A.; Jadoon, T.; Ayub, K. M@[12-crown-4] and M@[15-crown-5] where (M = Li, Na, and K); the very first examples of non-conventional one alkali metal-containing alkalides with remarkable static and dynamic NLO response. *Phys. E* **2022**, *140*, 115170.

(23) Ahsin, A.; Shah, A. B.; Ayub, K. Germanium-based superatom clusters as excess electron compounds with significant static and dynamic NLO response; a DFT study. *RSC Adv.* **2022**, *12*, 365−377.

(24) Ahsin, A.; Ayub, K. Theoretical Investigation of Superalkali Clusters M2OCN and M2NCO (where M= Li, Na, K) as Excess Electron System with Significant Static and Dynamic Nonlinear optical response. *Optik (Stuttg).* **2021**, *227*, 166037.

(25) Ahsin, A.; Ayub, K. Remarkable electronic and NLO properties of bimetallic superalkali clusters: a DFT study. *J. Nanostruct. Chem.* **2021**, *12*, 529−545.

(26) Sobczyk, M.; Simons, J. The role of excited Rydberg states in electron transfer dissociation. *J. Phys. Chem. B* **2006**, *110*, 7519−7527.

(27) Ullah, F.; Kosar, N.; Ayub, K.; Mahmood, T. Superalkalis as a source of diffuse excess electrons in newly designed inorganic electrides with remarkable nonlinear response and deep ultraviolet transparency: A DFT study. *Appl. Surf. Sci.* **2019**, *483*, 1118−1128.

(28) Liyanage, P. S.; de Silva, R. M.; de Silva, K. Nonlinear optical (NLO) properties of novel organometallic complexes: high accuracy density functional theory (DFT) calculations. *J. Mol. Struct.: THEOCHEM* **2003**, *639*, 195−201.

(29) Ellaboudy, A.; Dye, J. L.; Smith, P. B. Cesium 18-Crown-6 Compounds. A Crystalline Ceside and a Crystalline Electride. *J. Am. Chem. Soc.* **1983**, *105*, 6490−6491.

(30) Damjanović, M.; Morita, T.; Katoh, K.; Yamashita, M.; Enders, M. Ligand π-Radical Interaction with f-Shell Unpaired Electrons in Phthalocyaninato−Lanthanoid Single-Molecule Magnets: A Solution NMR Spectroscopic and DFT Study. *Chem. - Eur. J.* **2015**, *21*, 14421−14432.

(31) Jha, P. C.; Rinkevicius, Z.; Ågren, H. Spin multiplicity dependence of nonlinear optical properties. *ChemPhysChem* **2009**, *10*, 817−823.

(32) Nakano, M.; Nitta, T.; Yamaguchi, K.; Champagne, B.; Botek, E. Spin Multiplicity Effects on the Second Hyperpolarizability of an

https://doi.org/10.1021/acsomega.3c09468
ACS Omega 2024, 9, 14043−14053

Open-Shell Neutral π-Conjugated System. *J. Phys. Chem. A* **2004**, *108*, 4105−4111.
(33) Rezaee, M.; Rahman Setayesh, S. Theoretical study of the para chlorophenol adsorption on phosphorus-doped polypyrrole with DFT. *J. Chem. React. Synth.* **2022**, *12*, 1−13.
(34) Halium, E. M. F.; Mansour, H.; Alrasheedi, N.; Al-Hossainy, A. F. High-performance one and two-dimensional doped polypyrrole nanostructure for polymer solar cells applications. *J. Mater. Sci.: Mater. Electron.* **2022**, *33*, 10165−10182.
(35) Rajput, A.; Kulkarni, M.; Deshmukh, P.; Pingale, P.; Garkal, A.; Gandhi, S.; Butani, S. A key role by polymers in microneedle technology: a new era. *Drug Dev. Ind. Pharm.* **2022**, *47*, 1713−1732.
(36) Frisch, M. J.; Trucks, G. W.; Schlegel, H. B.; Scuseria, G. E.; Robb, M. A.; Cheeseman, J. R.; Scalmani, G.; Barone, V.; Mennucci, B.; Petersson, G. A.. *Gaussian* **2009**, *09*.
(37) Yanai, T.; Tew, D. P.; Handy, N. C. A New Hybrid Exchange−Correlation Functional Using the Coulomb-Attenuating Method (CAM-B3LYP). *Chem. Phys. Lett.* **2004**, *393*, 51−57.
(38) Limacher, P. A.; Mikkelsen, K. V.; Luthi, H. P. On the Accurate Calculation of Polarizabilities and Second Hyperpolarizabilities of Polyacetylene Oligomer Chains using the CAM-B3LYP Density Functional. *J. Chem. Phys.* **2009**, *130*, 194114.
(39) Paschoal, D.; Dos Santos, H. F. Assessing the quantum mechanical level of theory for prediction of linear and nonlinear optical properties of push-pull organic molecules. *J. Mol. Model.* **2013**, *19*, 2079−2090.
(40) Okuno, K.; Shigeta, Y.; Kishi, R.; Miyasaka, H.; Nakano, M. Tuned CAM-B3LYP functional in the time-dependent density functional theory scheme for excitation energies and properties of diarylethene derivatives. *J. Photochem. Photobiol. A Chem.* **2012**, *235*, 29−34.
(41) O'boyle, N. M.; Tenderholt, A. L.; Langner, K. M. cclib: A library for package independent computational chemistry algorithms. *J. Comput. Chem.* **2008**, *29*, 839−845.
(42) Tsuneda, T.; Song, J. W.; Suzuki, S.; Hirao, K. On Koopmans' theorem in density functional theory. *J. Chem. Phys.* **2010**, *133*..
(43) Ahsin, A.; Ali, A.; Ayub, K. Alkaline earth metals serving as source of excess electron for alkaline earth metals to impart large second and third order nonlinear optical response; a DFT study. *J. Mol. Graphics Modell.* **2020**, *101*, 107759.

https://doi.org/10.1021/acsomega.3c09468
ACS Omega 2024, 9, 14043−14053